Earth's Future

RESEARCH ARTICLE
10.1029/2022EF003347

How Extreme Events in China Would Be Affected by Global Warming—Insights From a Bias-Corrected CMIP6 Ensemble

Junhong Guo[1], Xiuquan Wang[2], Yurui Fan[3], Xi Liang[4], Hongtao Jia[1], and Lvliu Liu[5]

[1]MOE Key Laboratory of Resource and Environmental, System Optimization, College of Environmental Science and Engineering, North China Electric Power University, Beijing, China, [2]School of Climate Change and Adaptation, University of Prince Edward Island, Charlottetown, PE, Canada, [3]Department of Civil and Environmental Engineering, Brunel University, London, UK, [4]Sustainable Finance and Infrastructure Transition, Bartlett School of Sustainable Construction, University College London, London, UK, [5]Beijing Climate Centre, China Meteorological Administration, Beijing, China

Key Points:

- A downscaled and bias-corrected CMIP6 ensemble is used to evaluate the impact of global warming on ultra extreme events over China
- More frequent extreme hot-wet events with concurrence in the same month and year would be expected for China
- Both extreme hot events and extreme wet events would drop by above 25% from 2.0°C to 1.5°C global warming level

Supporting Information:

Supporting Information may be found in the online version of this article.

Correspondence to:

X. Wang and X. Liang,
xiuquan.wang@gmail.com;
xi.liang@ucl.ac.uk

Citation:

Guo, J., Wang, X., Fan, Y., Liang, X., Jia, H., & Liu, L. (2023). How extreme events in China would be affected by global warming—Insights from a bias-corrected CMIP6 ensemble. *Earth's Future*, *11*, e2022EF003347. https://doi.org/10.1029/2022EF003347

Received 15 NOV 2022
Accepted 13 MAR 2023

Abstract

In recent years, concurrent climate extreme conditions (i.e., hot-dry, cold-dry, hot-wet, and cold-wet) have led to various unprecedented natural disasters (e.g., floods, landslide, wildfire, droughts, etc.), causing significant damages to human societies and ecosystems. This is especially true for China where many unprecedented natural disasters have been reported due to the recent warming in local climate. In this paper, we focus on the issue of ultra-extreme events (1‰ threshold) and address how future global warming would affect the climate extreme conditions in China. Specifically, to reduce the uncertainties from models, we use a downscaled and bias-corrected CMIP6 ensemble under two continuously-warming scenarios to evaluate the impact of global warming on ultra-extreme events over China. The results show that, under both SSP245 and SSP585 scenarios, extreme hot conditions would become dominant in most regions of China and some regions are likely to experience over 50 extreme hot days at future warming levels. The frequency of extreme cold events is projected to be small. More frequent extreme hot-wet events with concurrence in the same month and year would be expected for China under the continuously-warming scenarios. This is particularly obvious for the west where more than 6 hot-wet months are likely to take place under future warming scenarios. This may imply that more extreme heat waves and flooding events would coincide in the same month or year for China in the future. For univariate ultra-extreme events, both extreme hot events and extreme wet events would drop by above 25% from 2.0°C to 1.5°C global warming level, particularly under the SSP245 scenario. When the global mean temperature is limited to 1.5°C rather than 2°C, the avoided impacts of hot-wet and cold-wet extremes concurring in the same month will be larger than those of dry-related compound extremes. Overall, the results suggest that slowing down global warming can reduce the frequency of concurrent climate extreme conditions in China, highlighting the importance of immediate action toward carbon emission reduction.

Plain Language Summary

In recent years, concurrent climate extreme conditions (e.g., hot-dry, cold-dry, hot-wet, and cold-wet) have led to various unprecedented natural disasters (e.g., floods, landslide, wildfire, droughts, etc.), causing significant damages to human societies and ecosystems. This is especially true for China where many unprecedented natural disasters have been reported due to the recent warming in local climate. In this paper, we focus on the issue of ultra-extreme events (1‰ threshold) and address how future global warming would affect the climate extreme conditions in China. Here, we use a downscaled and bias-corrected CMIP6 ensemble under two continuously-warming scenarios to address this question. The results show that, under both SSP245 and SSP585 scenarios, extreme hot conditions would become dominant in most regions of China and some regions are likely to experience over 50 extreme hot days at future warming levels. Both extreme hot events and extreme wet events would drop by above 25% from 2.0°C to 1.5°C global warming level, particularly under the SSP245 scenario. Overall, the results suggest that slowing down the global warming can reduce the frequency of concurrent climate extreme conditions in China, highlighting the importance of immediate action toward carbon emission reduction.

1. Introduction

The Paris Agreement adopted by 196 Parties at COP21 in 2015 set a global warming goal, which is to keep global warming to well below 2°C, preferably to 1.5°C, relative to the pre-industrial period (IPCC, 2018). To achieve this goal, every participating country has proposed its emission reduction roadmap and made the corresponding policies. As the largest developing country and one of the most carbon emitters, China proposed its target in

2020, called the "30·60 Dual-Carbon Target," that is, China will peak its carbon emissions by 2030 and neutralize carbon emissions by 2060 (You & Liu, 2022). This dual carbon target is essentially the same as the temperature control goals: endeavor to decrease global mean temperature and corresponding negative impacts.

With the intensification of global warming, it is recognized that the climate extremes in the aspect of duration, frequency and intensity are projected to increase and have profound impacts on the Earth system in the future (Shi et al., 2021). In general, extreme climate events have a deeper influence on human and natural systems than the climate mean state (Sun et al., 2016). Because climate changes have different impacts on geographically varying regions, changes in extreme events also show larger regional differences (Wang et al., 2013). With complex geographic patterns and various climatic characteristics, China is one of the most fragile countries to ongoing climate extremes. In the past several decades, enormous climate-related extreme events have led to tremendous losses of life and economy in China. For example, the most populous and economically-developed regions of China suffered from severe droughts in the summer of 2013 which resulted in tremendous economic losses and societal impacts (Zhou & Liu, 2018). In July 2021, Henan in China encountered a particularly severe flood event, causing 352 deaths and a cost of 16.5 billion $ (CRED, 2022). Therefore, robust and reliable information on future changes in temperature- or precipitation-dependent extremes is of paramount importance for making policy on climate change mitigation and adaptation.

Future information on climate change and related extremes can be projected by global climate models (GCMs). However, the spatial resolution of GCM is so imprecise that it is incapable to get detailed projections at the regional scale (Mishra et al., 2020), particularly for the areas with varied topography, and the simulated biases and uncertainties are larger in these models as well. Besides, due to the different resolutions, physical processes and forcing conditions, not all GCM models are equally plausible, in other words, there are more or few biases among models. In that case, the spread of models could be large if unrealistic models are involved in an ensemble (Tokarska et al., 2020). Even though the multi-model ensemble (MME) method can reduce the uncertainties from a single model to some extent, it may still increase the weight of the models with larger biases but decrease the proportion of the models with smaller biases. Relative to previous CMIP, the latest CMIP6 has larger improvements in spatial resolution, physical parameterizations and additional Earth system processes and components (Tian et al., 2021). Many studies in China have used the CMIP6 models to assess climate change and possible socio-economic impacts (Chen & Yuan, 2021; Guo et al., 2018; Su et al., 2021; Zhu et al., 2021).

To bridge the gap between the low-resolution GCM and the desire for detailed spatial projection at local regions, lots of dynamical and statistical downscaling methods are usually used to correct the biases of raw GCM. For dynamical methods, regional climate models (RCMs, i.e., WRF and RegCM, etc.) with physical mechanisms are developed to downscale the climatology in the local region (Li et al., 2021). However, one of the most shortcomings of RCMs is the cost of computing, due to the high consumption of computing and storage resources to run the RCMs at higher spatiotemporal resolution. On the other hand, the statistical downscaling method can provide a fast and efficient way to correct the biases in the original GCM, by building the mathematical relationship between fine-resolution observations and coarse-resolution climate variables (Yang et al., 2018). In this field, prior studies have developed various statistical approaches in this way from simple additive (Yang et al., 2018), linear-scaling (Zhu et al., 2022) to more sophisticated quantile mapping (QM) technologies (Ayugi et al., 2020; Enayati et al., 2021). Especially for the latter, the QM method is based on the cumulative distribution function (CDF) of reference data to correct the distribution of simulations, besides conventional mean and variance corrections (Wang & Chen, 2014). Generally, the QM has a premise that the statistical relationship (i.e., CDF) between the observation and the simulation will remain stable in the future period (Yang et al., 2018). However, it ignores potential changes in the CDF of meteorological variables under the background of future climate change (Guo et al., 2020). Thus, improved QM methods have been emerging to remediate this issue in recent years. Li et al. (2010) took into account the changes in meteorological fields under the future period and developed the equidistant cumulative distribution function matching (EDCDF) approach. Due to its virtue, this method has been widely used in the bias correction of climate simulations and projections (Piao et al., 2022; Yang et al., 2018).

Extreme climate events, though not frequent, often result in more severe ecologically and socioeconomically detrimental consequences (Ridder et al., 2020). Some extreme indices are used widely to represent the characteristics (intensity, frequency and duration) of climate extreme events, such as the Expert Team on Climate Change Detection and Indices (ETCCDI) (de los Milagros Skansi et al., 2013; Kim et al., 2020; Zhu et al., 2021). The ETCCDI consists of several temperature and precipitation extreme indices, which are based on an absolute or

Table 1
Timing of 1.5°C and 2°C Global Warming Above the Pre-Industrial Level (1850–1900) Under SSP245 and SSP585 Scenarios

	1.5°C		2.0°C	
CMIP6	SSP245	SSP585	SSP245	SSP585
ACESS-CM2	2028(2019–2038)	2025(2016–2036)	2040(2031–2050)	2038(2029–2048)
ACCESS-ESM1-5	2029(2020–2039)	2027(2018–2037)	2045(2036–2055)	2039(2030–2049)
BCC-CSM2-MR	2035(2026–2045)	2030(2021–2040)	2057(2048–2067)	2043(2034–2053)
CCCma-CanESM5	2013(2004–2023)	2012(2003–2022)	2024(2015–2034)	2022(2013–2032)
CNRM2	2037(2028–2047)	2032(2023–2042)	2055(2046–2065)	2045(2036–2055)
HadGEM3-GC31-LL	2013(2004–2023)	2020(2011–2030)	2033(2024–2043)	2029(2020–2039)
INM-CM4-8	2035(2026–2045)	2030(2021–2040)	2063(2054–2073)	2046(2037–2056)
INM-CM5-0	2037(2028–2047)	2030(2021–2040)	2072(2063–2082)	2046(2037–2056)
IPSL-CM6A-LR	2018(2009–2028)	2018(2009–2028)	2033(2024–2043)	2034(2025–2044)
MIROC6	2046(2037–2056)	2040(2031–2050)	2073(2064–2083)	2053(2044–2063)
MPI-ESM1-2-HR	2037(2028–2047)	2033(2024–2043)	2063(2054–2073)	2049(2040–2059)
MRI-ESM2-0	2030(2021–2040)	2026(2017–2036)	2049(2040–2059)	2038(2029–2048)

percentile threshold. Another extreme index is the Standardized Precipitation Index and it is often applied to characterize the climate drought or flood events at a spread of timescales (Liu et al., 2021; Sobral et al., 2019). For extreme temperature, some studies employed heat waves or cold waves indices to detect and describe the features of extreme-temperature anomalies (Morsy and El Afandi, 2021). On the other hand, when two or more extremes coincide, the resultant consequence would be even more harmful to human society and the natural environment (Xu & Luo, 2019). Thus, studies on the compound extremes which are a joint of multiple extreme climate events are also emerging and becoming a hotspot. For example, at a global scale, Meng et al. (2022) used the threshold of the 25th/75th percentile of precipitation and temperature to define the compound dry-warm events and compound wet-warm events. Zhang et al. (2020) analyzed comprehensively the spatio-temporal evolution of short-term concurrent hot-dry events at global and basin scales, and the results indicated that hot-dry events were found mostly in Northern Hemisphere regions with less precipitation. In China, Yu and Zhai (2020) created the CDHEEs index based on both day and night temperature over 90 percentile thresholds to explore the possible changing features of the compound drought and hot extreme events in eastern China. Lu et al. (2018) investigated how Compound Extreme Hot and Dry days (CEHD days) changes in the past and the response to future climate warming, and analyzed the impact of the CEHD on crops in China.

In summary, extensive studies have investigated the changes in the past and future climatology, including the climatic mean state and extreme events under different global warming scenarios, particularly for the compound extremes, its characteristics of more serious consequences are destined to become one of research highlights. Through referring to the current studies, we found that though the definition of the extreme indices or concurrent extremes is various, they are basically based on a threshold of a preference period. The percentile threshold is one of most used in studies, such as exceeding the 90th percentile or less than the 10th percentile. To the best of our knowledge, the study on very extreme or ultra-extreme events, that is, the threshold which is 99.9% or 0.1% is very limited. Thus, in this study, we have developed a bias-corrected and high-resolution model ensemble based on the 12 CMIP6 models and analyzed the changes in the temperature- and precipitation-related ultra-extreme events in China at the two different global warming levels. In particular, the target of our study is mainly to address the following questions: (a) How will ultra extremes change in China under the different global warming levels and emission scenarios? (b) To what extent the impacts of ultra-extreme events in China could be avoided if global warming is limited to 1.5°C rather than 2°C?

2. Data and Methods

2.1. Data

Climate model data consist of original data and corresponding bias-corrected outputs of 12 CMIP6 models (Table 1) in the historical period of 1995–2014, and in the future period of 2015–2100 under SSP2-RCP4.5

(SSP245) and SSP5-RCP8.5 (SSP585) emission scenarios. The observed daily maximum temperature, daily minimum temperature and daily precipitation in China are from a data set of CN05.1, which is developed by the China Meteorological Administration. This data set has a spatial resolution of 0.25° × 0.25° by interpolating above 2,400 weather stations in China. It has been widely used in various hydroclimatic applications (Jia & Xue-Jie, 2013; Ying-Xue et al., 2020). Here, we employ it to downscale the raw CMIP6 models and validate the performance after bias correction. In addition, the output of the MME mean is obtained by averaging meteorological variable statistics calculated from different climate models with distinct periods and scenarios.

2.2. Downscaling and Bias Correction

The overall procedure of downscaling and bias correction is divided into two parts:
First, for each month, the mean observed meteorological variables (i.e., daily maximum, minimum temperature and daily precipitation) in the historical period are interpolated at the same resolution with the CMIP6 model, respectively. Second, we calculate the differences between the interpolated observation and each GCM. Third, these anomaly fields are further interpolated to the original resolution and then add to the observed variables to generate the downscaled output for each GCM. All interpolation processes use a bilinear interpolating technology. The EDCDF is used to correct the biases from the downscaled CMIP6 models. This method is an improved QM technology, which can adjust the CDF of a model simulation to match that of observed values instead of correcting the mean and variance of model output (Wang & Chen, 2014). There is an underlying assumption that the discrepancies between the simulated values and the observation in the historical or baseline period are in line with those in the future period for a given percentile (Tian et al., 2021; Wei et al., 2022; Yang et al., 2022).

In this paper, the daily temperature and precipitation series are fitted based on the normal distribution and mixed gamma distribution. This approach is defined as follows:

$$\tilde{x}_{m-p} = x_{m-p} + F_{o-c}^{-1}(F_{m-p}(x_{m-p})) - F_{m-c}^{-1}(F_{m-p}(x_{m-p})) \quad (1)$$

where $\tilde{x}_{m-p}$ is corrected daily maximum and minimum temperature and daily precipitation from CMIP6 in the future period; x_{m-p} is the projected raw climatic variables; F_{m-p} refers to the CDF of the GCM projection in the future period; F_{o-c}^{-1} and F_{m-c}^{-1} are the distribution functions (inverse CDF) for observation and models in the reference period, respectively.

2.3. Definition of Indices and Global Warming Levels

Following the method of a previous study (Vogel et al., 2020), we define the ultra-extreme events with a 1‰ likelihood of occurrence in the baseline period. In other words, the extreme event occurs when the climatology variable value is above or below a quantile-based threshold (99.9% or 0.1%). Four ultra-extreme indices are considered in this paper: hot extremes, cold extremes, wet extremes and dry extremes. Hot and cold extremes are calculated based on the daily maximum and minimum temperature. For each grid of model, the 99.9th (0.1th) percentile of maximum (minimum) temperature in the baseline period is computed first. Then the number of hot (cold) extreme events is tallied by counting the days of exceedances over/below the 99.9th (0.1th) threshold at different warming levels. On the other hand, the daily precipitation is aggregated through a running 5-day (run5) and 90-day (run90) window in the baseline and future periods, respectively. Then the 99.9th (0.1th) percentile of precipitation of run5 (run90) in the baseline period is determined. We define the wet (dry) extreme event as a day where precipitation is higher (lower) than the 99.9th (0.1th) percentile at different warming levels. Likewise, the number of wet and dry events is countered afterward. Through combination with each other, four types of concurrent extremes are defined, which are hot-wet, hot-dry, cold-wet and cold-dry extreme events, respectively. The probabilities of occurrence of these compound events are further analyzed in different time scales at each grid, that is, in the same month and year.

The arrival timing of 1.5°C and 2.0°C warming levels relative to the pre-industrial period (1850–1900) is determined for each member of CMIP6 under different SSP scenarios. First, the global mean surface temperature is averaged in a 20-year running window. Then, the threshold year is determined when the global mean temperature reaches 1.5°C or 2.0°C relative to the pre-industrial level (Kim & Bae, 2021; Tang et al., 2022; Zhao et al., 2021). Finally, a 20-year period extending from 9 years prior and 10 years after the threshold year is as the future projection period at different warming levels and scenarios (Table 1). Moreover, the period (1995–2014) with the same

20-year length is as the historical or reference period to validate the performance of each GCM and calculate the extreme indices in the future. The avoided impact of temperature and precipitation indices at an extra 0.5°C warming level is computed as follows (Li et al., 2018, 2021):

$$\mathrm{AI} = \frac{\Delta V_{2.0} - \Delta V_{1.5}}{\Delta V_{2.0}} \times 100\% \tag{2}$$

Here, AI represents the avoided impact, $\Delta V_{2.0}$ and $\Delta V_{1.5}$ show the differences in temperature or precipitation indices between the 2.0°C and 1.5°C relative to the baseline simulation, respectively.

2.4. Taylor Diagram and Skill Score

To quantify the agreement on the spatial pattern of the historical climate variables between observations and model simulations, the Taylor diagram (Taylor, 2001) is applied in this paper. Taylor diagram can provide three skill indicators: spatial correlation coefficient (R), centered pattern root-mean-square error (CRMSE), and the ratio of spatial standard deviation (RSD). There is a reference point (REF) in its axis as the observation. The angular axes of the diagram indicate spatial correlations between modeled and observed values. The value of radial axes shows spatial standard deviation. The closer to the REF arc the model point is, the higher reproducing the ratio spatial standard deviation of observation is. The distance between the model and the REF point represents the centered pattern root-mean-square error against the observations. A good simulation would be that both the spatial correlation and ratio of spatial standard deviations are close to 1 and the centered pattern-root mean-square error is equal to 0 (Jiang et al., 2015). Additionally, to evaluate comprehensively above three performance skills from the Taylor diagram, a skill score is used (Chen & Frauenfeld, 2014; Hirota & Takayabu, 2013):

$$S = \frac{(1+R)^4}{4(\mathrm{RSD} + 1/\mathrm{RSD})^2} \tag{3}$$

where S is the Taylor skill score. The score is higher and the performance is better.

3. Results

3.1. Model Evaluation

In spatial distribution, the output from CMIP6 multi-model mean exhibits outstanding performance in reproducing the historical climatology patterns over China (Figure 1). The major hot and cold centers in simulations compare well against CN05.1. The bias-corrected simulations are evidently better than the raw CMIP6 simulations in capturing the maximum temperature in northwestern China. In addition, the spatial distribution in the minimum temperature of the CMIP6 ensemble after correction is in accordance with the observation relative to the raw models. For both CMIP6 simulations, the annual precipitation shows an apparent feature in the spatial pattern, which is higher in the south and lower in the northwest. However, it is noted that the annual precipitation simulated by the original CMIP6 seems to have an artificial precipitation center in the Tibet Plateau compared with the CN05.1.

We assessed the MME mean bias of the above climate variables from the 12 CMIP6 GCMs against the observation CN05.1 in spatial distribution (Figure 2). For the maximum temperature, the raw CMIP6 GCMs show a warm bias (~4°C) in the northwest of China, while the southeast is underestimated by ~–3°C. Through bias correction, these biases are substantially reduced during the historical period over China, with a bias ranging from −1–1°C. The original CMIP6 ensemble shows an obvious underestimation in simulating the minimum temperature, especially for the west and eastward regions, where the simulated minimum temperature is totally lower (even exceeding 5%) than the observation. Although the corrected result still has a slight cold bias compared with the CN05.1, the improvement is enormous relative to the no-correction CMIP6 ensemble. Additional evidence of the necessity for bias correction is from the results of precipitation. The overall precipitation simulated by raw CMIP6 over China is overvalued completely, particularly for the west, even more than 80% relative to the CN05.1. These wet biases are reduced to ~20% in the process of bias correction.

Figure 3 shows the Taylor diagrams for evaluating the ability of CMIP6 models in simulating the spatial pattern of three climate variables. Against the observations, the majority of raw CMIP6 models (red spots) have a

10.1029/2022EF003347

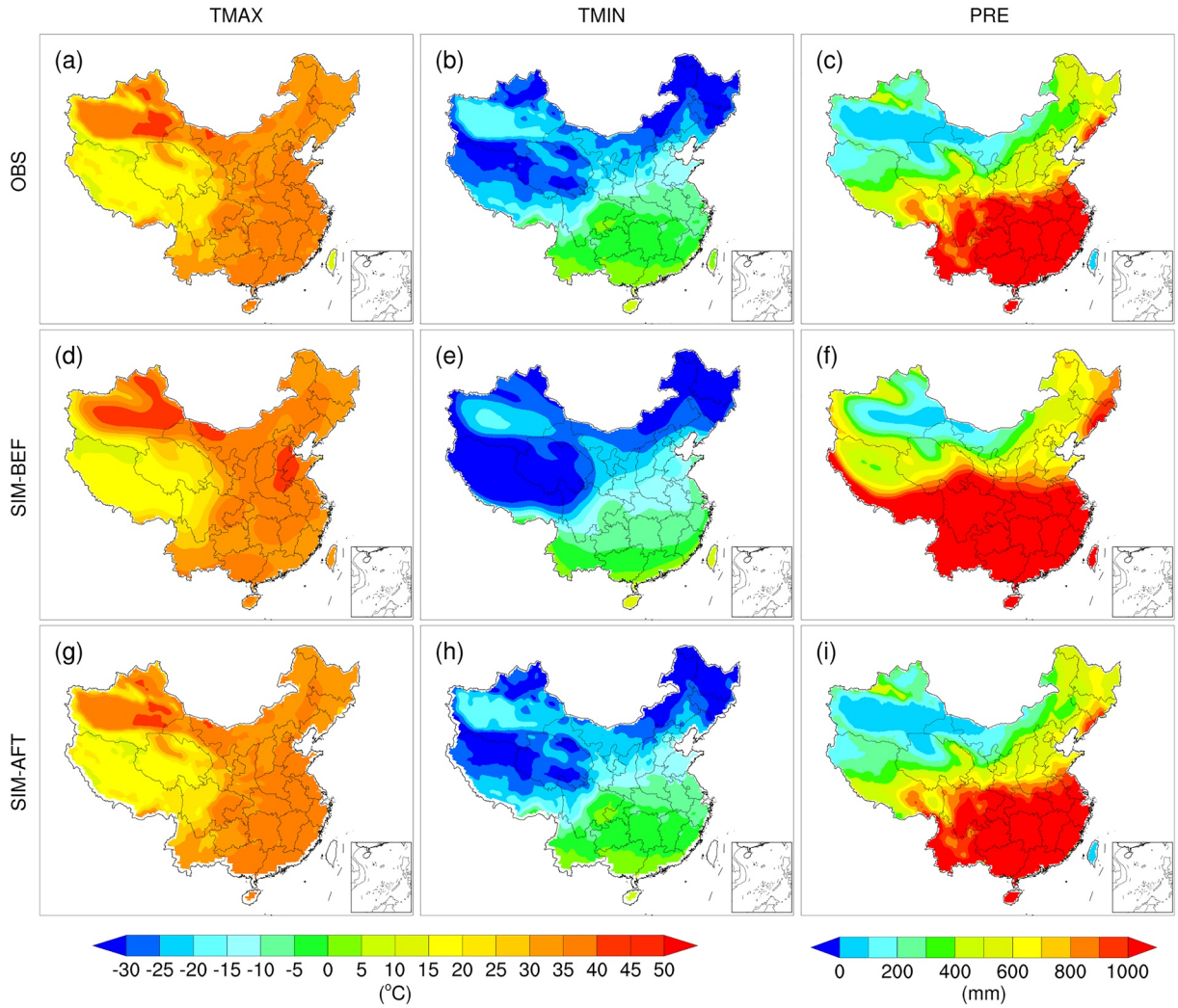

Figure 1. Spatial patterns for the climatological mean maximum temperature, minimum temperature and precipitation over China during 1995–2014. The rows from top to bottom indicate the results from the CN05.1, raw CMIP6, and bias-corrected CMIP6, respectively.

spatial correlation between 0.8 and 0.99 for annual maximum and minimum temperature, and about 0.6–0.9 for annual precipitation, while the values (blue spots) are above 0.99 through bias correction, indicating the corrected-bias models have a reasonable spatial correction with observation. Additionally, more than half of raw models have a ratio of variance larger than 1.0 and even exceeding 1.5 in simulating the annual precipitation, suggesting that the spatial variation in simulation is larger than observation over China, while these biases are corrected in improved CMIP6 models. As for the centered normalized root mean square error, the value in simulations from bias correction is below 0.25, which is smaller than the original models, even exceeding 0.75 for precipitation, indicating that the corrected models have a lower amplitude of biases. Moreover, the centralized distribution in the bias-corrected simulations for all variables indicates a smaller inter-model spread, while the much larger inter-model range in the raw CMIP6 models is found owing to the loosely scattered distribution in the Taylor diagram, particularly for the annual precipitation. In other words, large uncertainties among CMIP6 models are reduced during the procedure of bias correction.

To further provide an overall evaluation of the simulation skill from above Taylor diagram in each CMIP6 model before and after bias correction over China, the Taylor Score (TS) is employed in this study (Figure 4). It is clear that all the bias-corrected CMIP6 models show a good performance in simulating the spatial distribution of these variables with above 0.97 TS values. The scores of bias-corrected ensemble mean are raised to 0.993, 0.994, and 0.996 from 0.872, 0.898, and 0.703 before correction for the maximum temperature, minimum temperature and

10.1029/2022EF003347

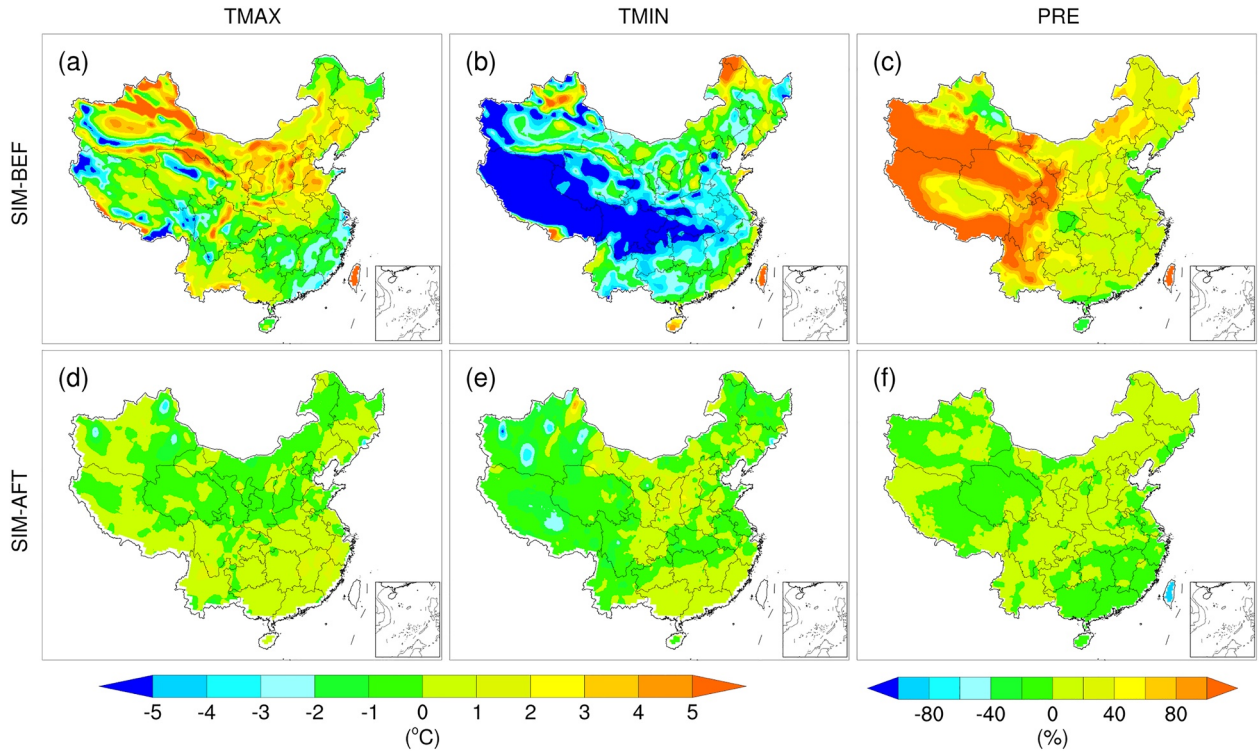

Figure 2. Multi-model ensemble mean bias in maximum temperature, minimum temperature and precipitation for the historical period (1995–2014). (a–c) Are biases before the bias correction, (d–f) are biases after bias correction.

precipitation, respectively. Especially for the annual precipitation, the improvement after bias correction is more obvious due to a large increase in TS values.

In addition, the comparisons in extreme percentile thresholds between observation, raw model and bias-corrected model are analyzed (Figure S1 in Supporting Information S1), and the biases before and after correction are shown in Figure S2 in Supporting Information S1. Overall, the simulated percentile thresholds of four extreme indices in spatial distribution are consistent with observation, although the magnitude of bias varies before and after correction. The biases of simulations relative to the observation show that the superiority of bias correction is evident. The differences of original CMIP6 models with the CN05 observed values are larger for most indices. For raw models, most regions present a colder temperature than observation in calculating the percentile threshold of extreme cold events, while these models overestimate the extreme wet threshold. After correction, the entire biases are remarkably reduced for both temperature and precipitation extreme thresholds.

The days of occurrence for four extreme indices over China in the baseline period are further calculated (Table S1 in Supporting Information S1). Theoretically, the number of extreme events under the 0.1% or 99.9% threshold in the 20-year historical period will be about 7.3 days (365*20*0.001), which means the extreme events for each grid over China should be close to this desired value. It is noted that the number of extreme dry events could be more than above value due to the number of non-precipitation days. The results show that the simulated days of extreme hot, cold and wet in the baseline period are essentially in agreement with the observation, while the bias-corrected results have a smaller bias in calculating the days of extreme dry events.

3.2. Projections at Specified Warming Levels

3.2.1. Changes in Mean Climatology

Figures 5 and 6 depict the changes in annual maximum temperature, minimum temperature and precipitation over China at two global warming levels under SSP245 and SSP585 emission scenarios. Table 2 shows the corresponding results of the regional mean. Under SSP245, compared with the historical period, both annual maximum and minimum temperature will increase and the former exhibits a larger magnitude. On the whole of China, the maximum temperature is likely to increase by 1.43°C and 1.97°C, while the regional mean minimum

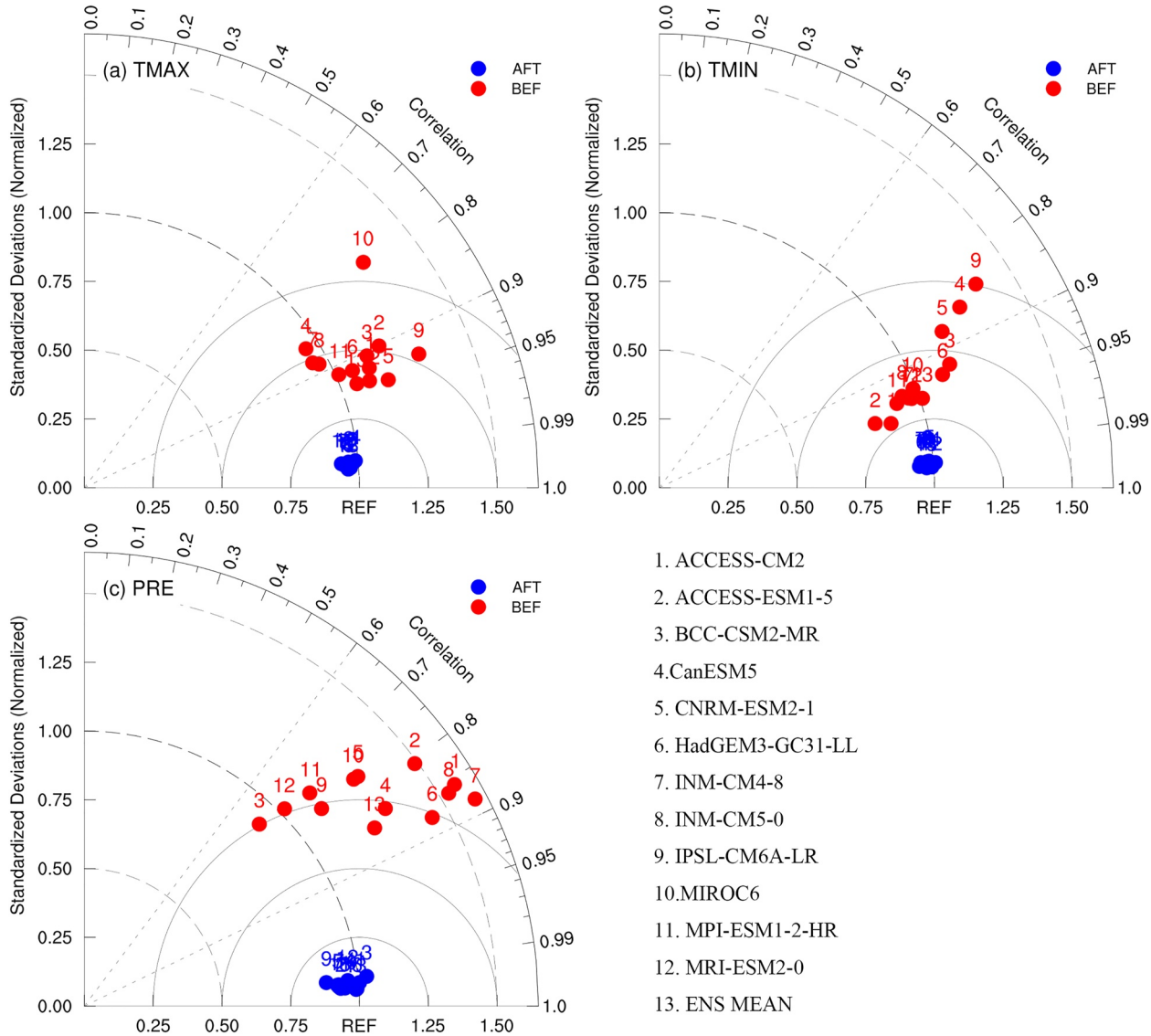

Figure 3. Taylor diagrams of the annual maximum temperature, minimum temperature and precipitation between observation and 12 models and ensemble mean before (red) and after (blue) bias correction over China.

temperature is projected to rise by 1.02°C and 1.83°C at 1.5°C and 2.0°C global warming levels under SSP245 scenario. However, the changes in spatial distribution are different between annual maximum and minimum temperature. Specifically, the changes in annual maximum temperature are larger in northwest Tibet, while the northeast and central China show a larger increasing trend than other regions. It is noted that the magnitude and spatial scope of the increase in annual minimum temperature with an additional 0.5°C warming are larger than the maximum temperature, even exceeding 1.5°C in some regions. Overall, compared to the baseline period of 1995–2014, the annual precipitation over China will increase by 10.66% and 15.38% under 1.5°C and 2°C global warming under SSP245. In spatial distribution, except for the northwest, the magnitude of precipitation increase over western China will be larger than that in the south, particularly for the south of Xinjiang and the west of Tibet, even more than 20% compared with the baseline. The largest increase in annual precipitation with an extra 0.5°C warming is largely focused over the southwest of Xinjiang, Beijing-Tianjin-Hebei and Shandong regions.

Compared to the baseline period, the changes in the spatial distribution of three climate variables under the SSP585 scenario are similar to those under SSP245 but with a larger increasing magnitude. Under an extra 0.5°C warming, the minimum temperature and precipitation are projected to have a smaller increase under SSP585 than that under SSP245. For example, the area-averaged annual minimum temperature will increase by 0.8°C

10.1029/2022EF003347

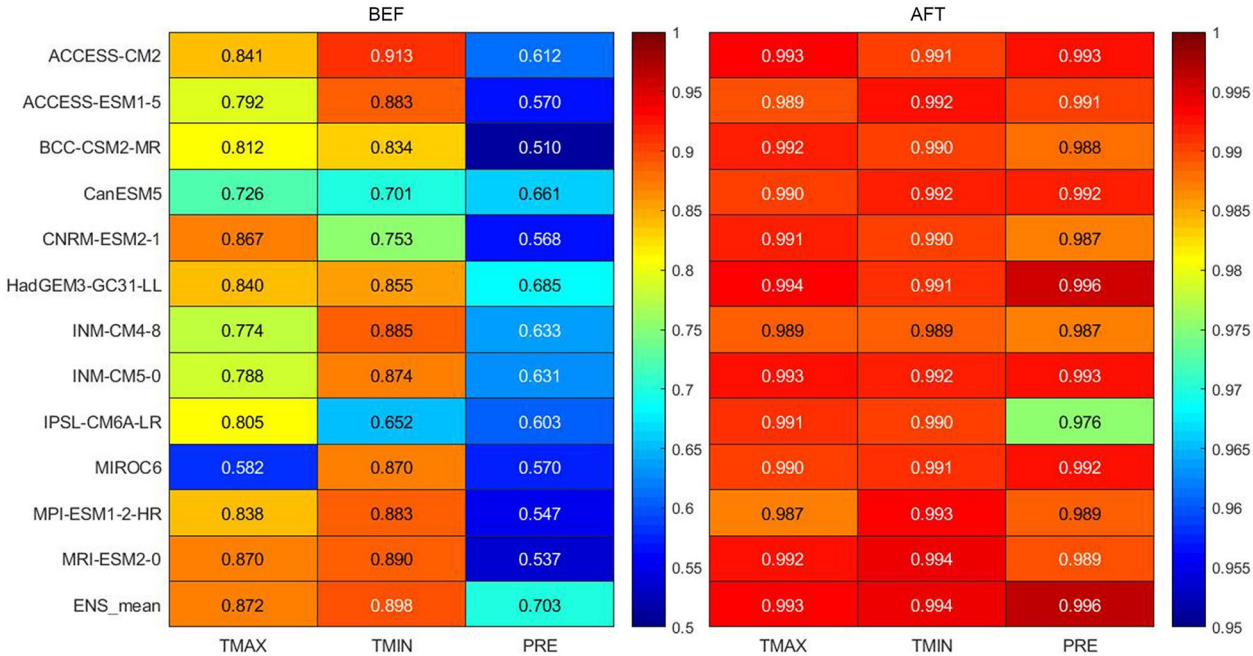

Figure 4. Taylor Score of the CMIP6 ensemble in simulating the spatial patterns of the maximum temperature, minimum temperature and precipitation during 1995–2014.

from 1.5°C to 2.0°C under SSP245, while the value will be reduced to 0.61°C under SSP585. In other words, the increment of minimum temperature and precipitation with an extra 0.5°C under a high-emission scenario is smaller than that under a lower emission.

3.2.2. Future Frequency of Extreme Events

The future frequency of four univariate extreme events at two global warming levels under different SSP scenarios is presented in Figure 7. Under the 1.5°C and 2.0°C global warming levels, extreme hot events will be dominated in most regions of China, where the frequency of occurring extreme hot weather will be above 50 days in some regions. A stronger increase is observed with increasing emissions and warming levels, even more than 100 days under SSP585 scenario at the 2.0°C warming level. Theoretically, the expected univariate extreme temperature or precipitation events in the baseline period (1995–2014) are about 8 days (1‰*365*20). That means future extreme hot events at a higher warming level and emission scenario will increase by more than 10 times compared with the baseline period. Owing to global warming, though future cold extremes can be expected to be found in China, its probability of occurrence is smaller than other indices. The north of China and Tibet region will experience about 8–10 days of extreme cold events in future global warming scenarios. However, the projected increase of extreme cold days will further shrink at a higher warming level, particularly in the north of China. Projected extreme dry events can reach about 20 days in total for most regions of China. The maximum occurrence frequency for dry extremes will be found in the west of Xinjiang, the southwest of Tibet and southern Sichuan. Most parts of China are likely to experience more extreme wet events with 30–40 days approximately. This probability of occurring the extreme wet events reaches 5 times larger compared to the reference period and is larger than that of dry events. In spatial distribution, the southeast of Xinjiang and northwest of Tibet are likely to occur more extreme wet events under 1.5°C and 2.0°C global warming.

Four compound variables, namely in the same month concurrent extreme hot-dry events, extreme hot-wet events, extreme cold-dry events, and extreme cold-wet events, are analyzed (Figure 8). Overall, the probability of concurrence of two extreme events is fairly smaller than that of single ones. Nevertheless, the results show that a great possibility for co-occurred extremes over China is the clustered extreme hot-wet events, particularly in the west of China, where monthly hot-wet events tend to experience above 6 under future global warming levels and emission scenarios. Additionally, a higher global warming level will result in a strong increasing magnitude. For example, the number of extreme hot-wet events with concurrence in the same month in northwest Tibet is likely

10.1029/2022EF003347

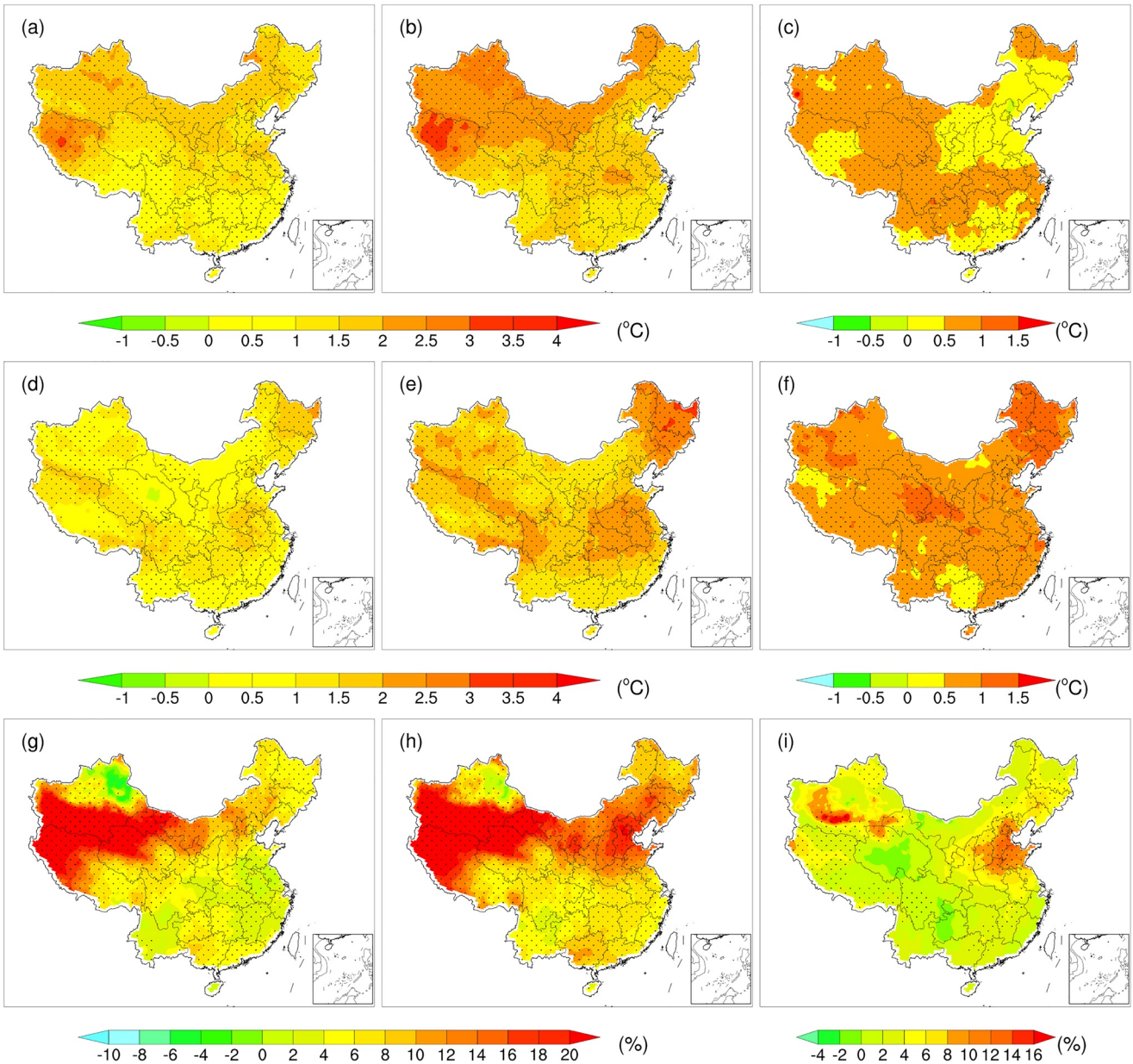

Figure 5. Spatial patterns for the changes in maximum temperature, minimum temperature and precipitation in 1.5°C and 2°C global warming levels from the CMIP6 models under SSP245 scenario (relative to the period of 1995–2014) over China. The right column shows the results due to an increase of 0.5°C. The light gray dot area indicates the statistical test with a Student-*t* statistical significance level of 5%.

to be up to 10 months at the 2.0°C warming level under the SSP585. On the other hand, in the same month, the frequency of occurrence for other clustered extremes is small in most parts of China (about 0.1–0.2 months). For the hot-dry events, only a few regional hotspots in Xinjiang are projected to exceed 0.5 months. Likewise, the numbers of concurrence for the two minimum daily temperature-related compound events are quite small across the whole of China. The extreme cold-dry/wet events in the same month mainly are found in the southern and western margins of Tibet.

Figure 9 presents the concurrence of four joint extreme events in the same year at two warming levels under SSP emission scenarios. It is easy to understand that the probability of co-occurring compound extremes in the same year is larger than that in the same month. The results describe that the most compound extreme event that occurs in the same year is the hot and wet extremes, which is similar to the results from the same month. At a

10.1029/2022EF003347

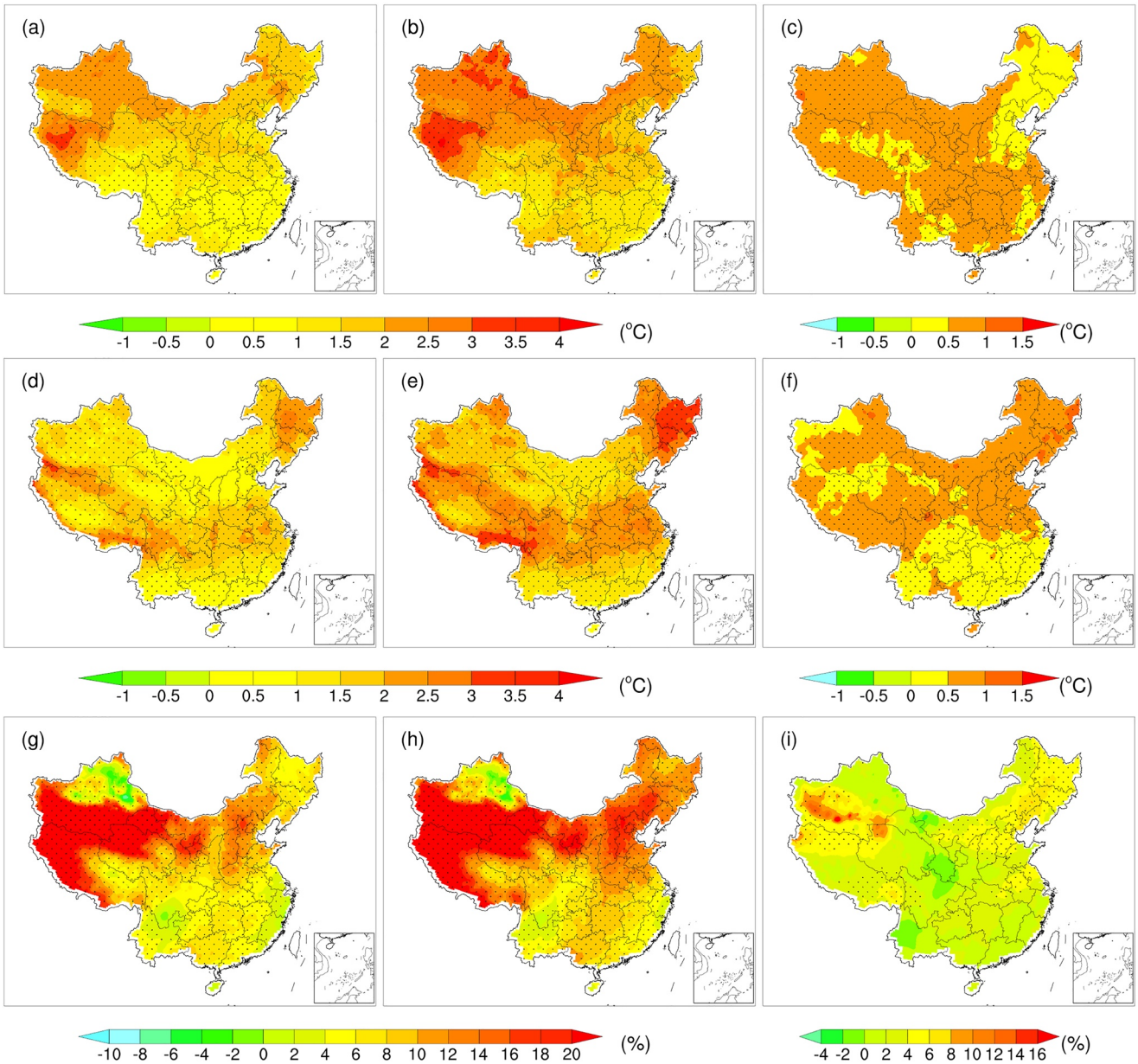

Figure 6. Spatial patterns for the changes in maximum temperature, minimum temperature and precipitation in 1.5°C and 2°C global warming levels from the CMIP6 models under SSP585 scenario (relative to the period of 1995–2014) over China. The right column shows the results due toan increase of 0.5°C. The light gray dot area indicates the statistical test with a Student-*t* statistical significance level of 5%.

Table 2
Regional Mean Changes in Maximum and Minimum Temperature and Precipitation Over China at Different Global Warming Levels Under SSP245 and SSP585 (in Brackets) Emission Scenarios

Warming levels	TMAX (°C)	TMIN (°C)	PRE (%)
1.5°C	1.43 (1.56)	1.02 (1.44)	10.66 (13.27)
2.0°C	1.97 (2.12)	1.83 (2.06)	15.38 (16.48)
△0.5°C	0.54 (0.56)	0.80 (0.61)	3.71 (3.21)

Note. The changes are significant statistically at a confidence level of 0. 95.

1.5°C warming, about 2–4 yearly clusters of extreme hot-wet events would occur over China, and up to 3–5 years with joint hot-dry extremes tend to be observed at the 2.0°C warming level. For joint extreme hot and dry events in the same year, the number of events is larger than that in the same month, suggesting that the extreme hot-dry events are likely to coincide within the same year but these events could hardly occur in the same month. The maximum number of extreme hot-dry events in the same year is around 3 in the future global warming period over the margin regions of western China. Compared with the hot-related compound indices, the probability of concurrence for cold-dry and cold-wet events in the same year is very limited, especially for the cold and dry extremes, the concurrent probability of the coldest

10.1029/2022EF003347

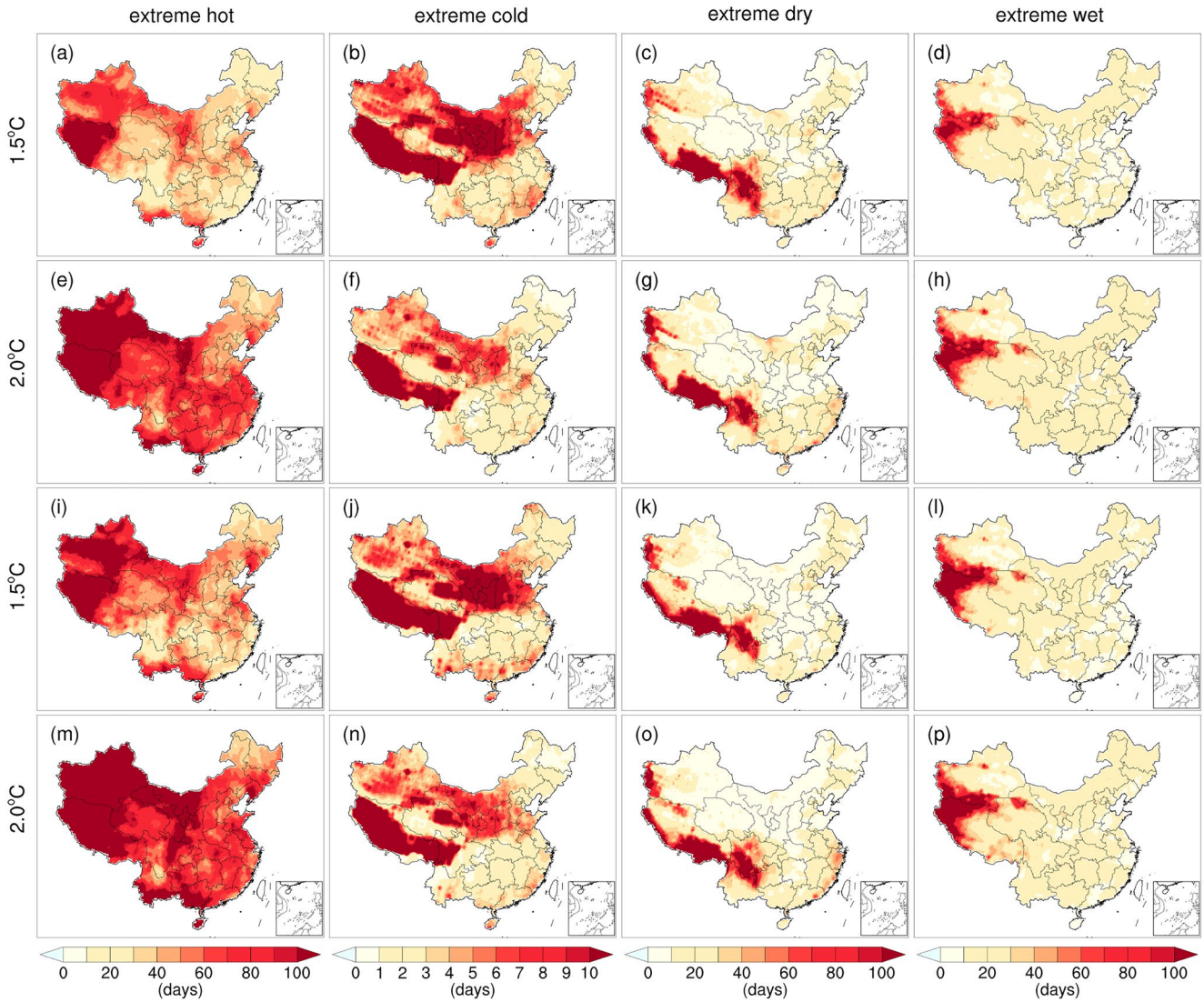

Figure 7. Occurrence of univariate extreme events at different warming levels under SSP245 (the first and second rows) and SSP585 (the third and fourth rows) scenarios. The columns from left to right are the extreme hot, extreme cold, extreme dry and extreme wet events, respectively.

and driest extreme events could be marginal in both the same year and month. In the west of China, there is only 1 year on average with cold-wet concurrent extreme events in the future.

3.2.3. Avoided Impacts

The avoided impacts of the maximum temperature, minimum temperature, precipitation and the corresponding extreme indices in China from 2.0°C to 1.5°C warming levels are further analyzed (Figure 10 and Table 3). Overall, though there are differences among CMIP6 models, most models show that there are largely avoided impacts under both future emission scenarios. If global warming is kept at 1.5°C rather than 2°C, the avoided impacts of three climate variables will exceed 25%, except for the precipitation under SSP585 scenario (23.3%). For the univariate extreme events, the avoided impacts for extreme hot events and extreme wet events are also above 25%, particularly for the extreme hot events, the regional mean result is even more than 50%, with 54.26% and 50.18% under SSP245 and SSP585 scenarios, respectively. It means that the occurrence of extreme hot events over China would decrease more obviously compared with other univariate extremes when global warming is kept at 1.5°C. In other words, when global warming decreases by 25% (from 2.0°C to 1.5°C), the reduced extreme hot events will be far higher than this percentage. In the same month, the avoided impacts of wet-related extremes will be larger than those of dry-related compound extremes, while the concurrent cold-dry extreme events have

10.1029/2022EF003347

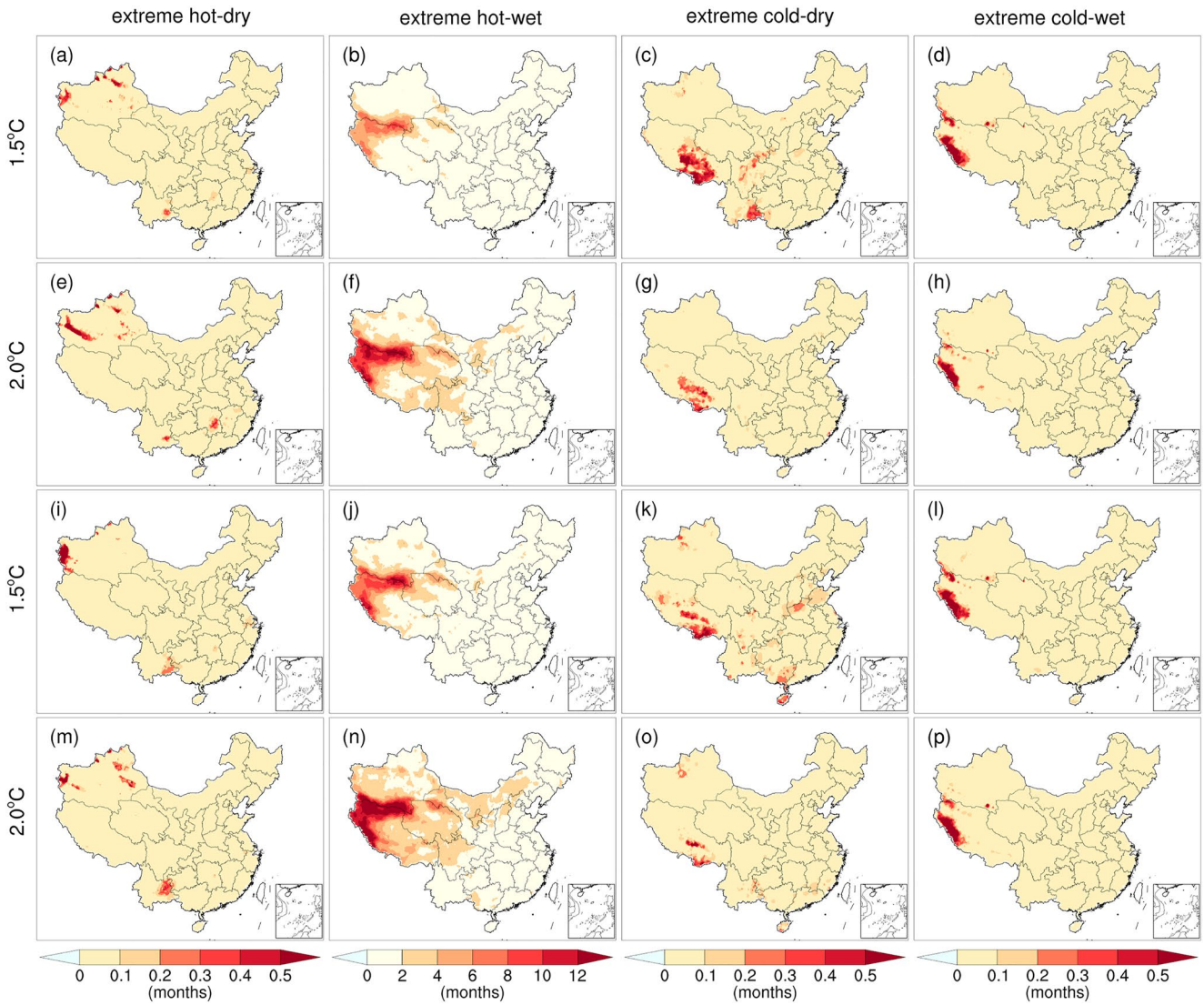

Figure 8. Concurrence of compound extreme events in the same month at different warming levels under SSP245 (the first and second rows) and SSP585 (the third and fourth rows) scenarios. The columns from left to right are the extreme hot and dry, extreme hot and wet, extreme cold and dry, and extreme cold and wet events, respectively.

less influence (only 13.27% under SSP585) on the added 0.5°C warming. On the other hand, the avoided impact from 0.5°C less warming for the concurrence of hot-dry extremes in the same year is higher than other compound indices. Likewise, the avoided changes of concurrent cold-dry extreme events are smaller in the same year.

In view of uncertainties, the CMIP6 models show a larger spread in analyzing the avoided impacts for the temperature-related indices, such as extreme hot and extreme cold events. For the compound extreme indices, the uncertainties of avoided impacts among models in the same month are more than those in the same year, especially for the hot-dry and cold-wet extreme events.

3.2.4. Comparison With Different Extreme Threshold

In this section, we analyzed and compared the results of extreme events defined by the thresholds 99% (1%) with very extreme or ultra-extreme events. The univariate and compound extreme indices in spatial under different emission scenarios and warming levels are shown in Figures S3–S5 (see the Supporting Information S1). Overall, the occurrence of univariate or compound extreme events defined with the 99% (1%) threshold in spatial distribution is similar with the ultra-extreme events. However, owing to more extreme thresholds, the possibility of occurrence for ultra-extreme events are smaller in terms of the number and regional scope of occurrence,

10.1029/2022EF003347

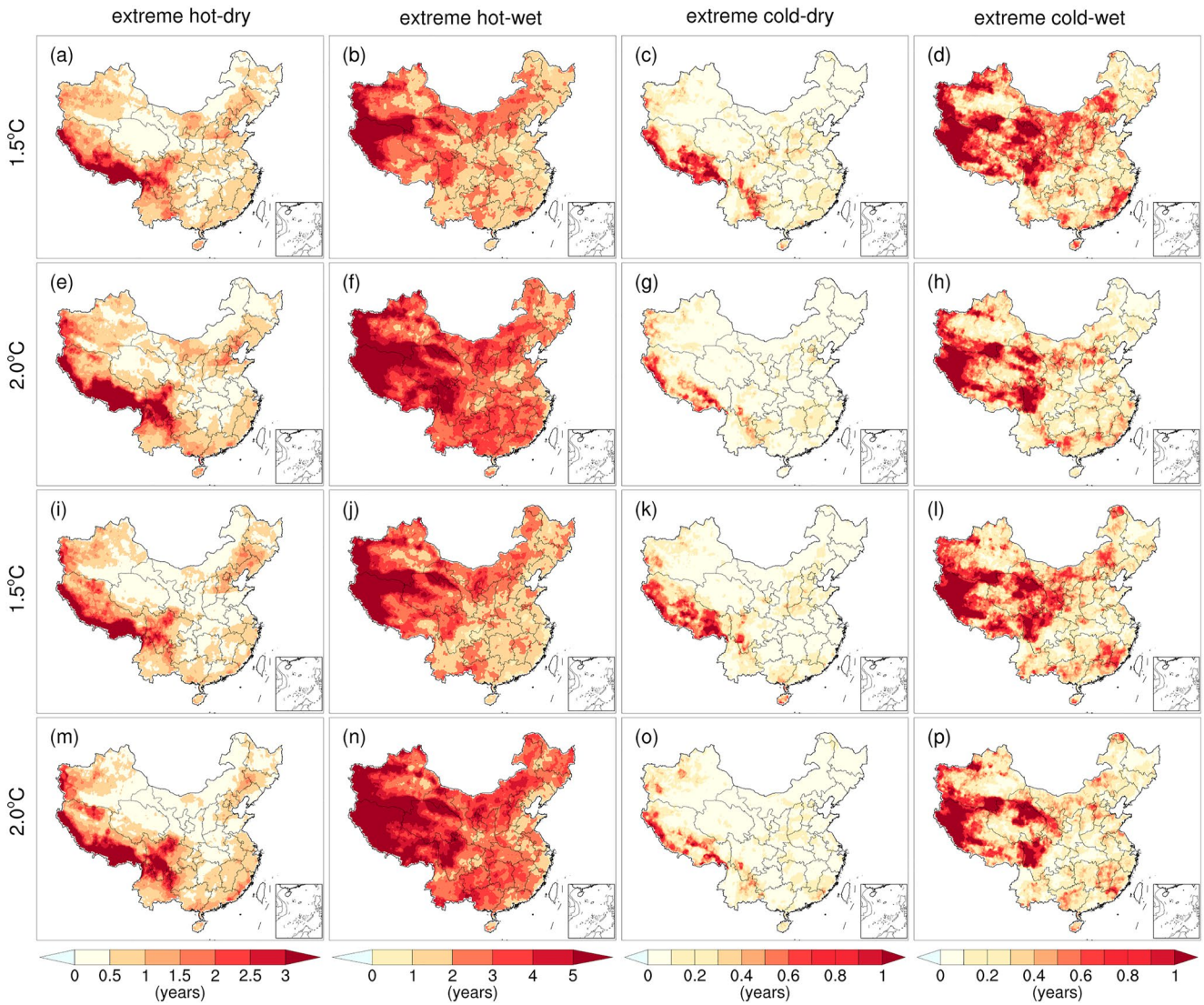

Figure 9. Concurrence of compound extreme events in the same year at different warming levels under SSP245 (the first and second rows) and SSP585 (the third and fourth rows) scenarios. The columns from left to right are the extreme hot and dry, extreme hot and wet, extreme cold and dry, and extreme cold and wet events, respectively.

especially for the concurrence of compound extreme events in the same month or year. Specifically, compared with the ultra extremes, the hot-dry and cold-dry extreme events defined with the 99% (1%) threshold are likely to occur in a month or year more frequently in the southern regions of China, while these ultra-extreme events are mainly found in the northwest. On the other hand, most regions in China are expected to suffer more hot-wet extreme events defined with the 99% (1%) threshold in a month or year compared with ultra-extreme events.

The regional mean avoided impacts of the univariate and compound extreme indices are calculated for two different percentile thresholds (Table S1 in Supporting Information S1). The results show that most univariate ultra-extreme indices have larger avoided impacts, suggesting the risk resulting from very extreme events would be avoided if global warming is reduced from 2.0°C to 1.5°C. In other words, although the frequency of occurrence for ultra-extreme events is small, the avoided impacts are larger than the extremes defined with the 99% (1%) threshold. On the other hand, the avoided impacts of ultra-extreme events are mainly found in projections on the hot-related compound extreme indices, that is, the hot-dry and hot-wet extremes. With the 99% (1%) threshold, the impacts of extreme cold-dry compound extreme are smaller than the ultra-extreme events under an additional 0.5°C warming scenario.

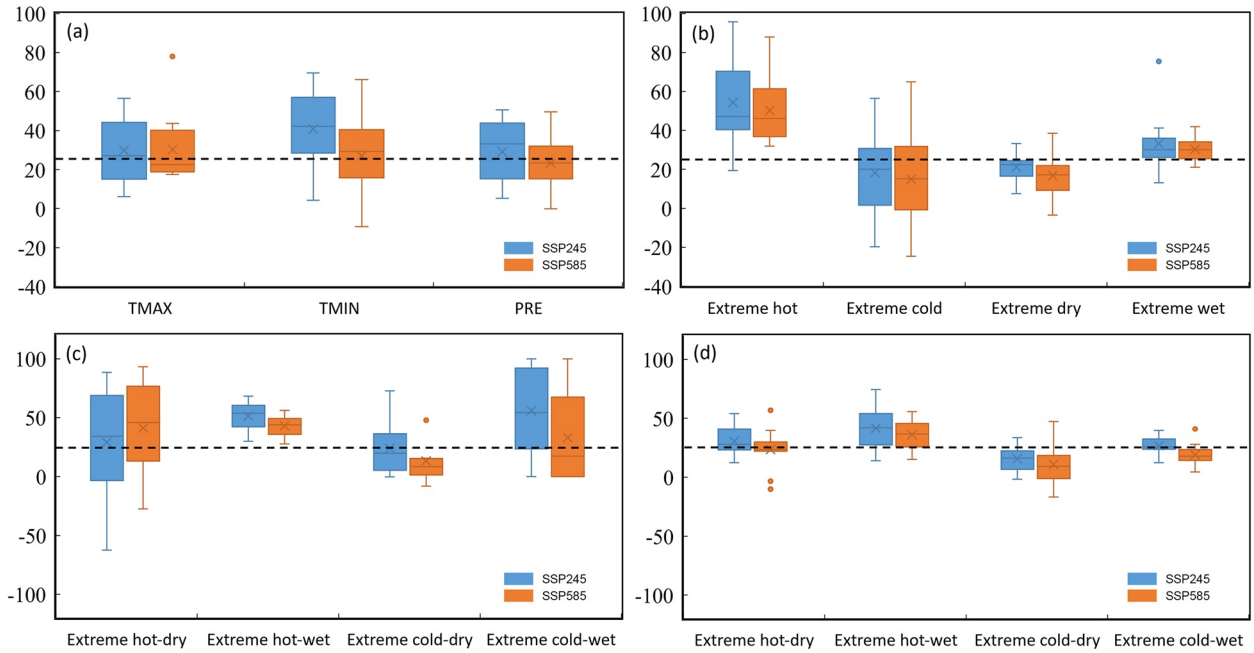

Figure 10. The avoided impacts (unit: %) of the maximum temperature, minimum temperature, precipitation and the corresponding extreme indices from 0.5°C less warming over China under SSP245 and SSP585 scenarios. Box plots show the inter-model spread and the cross depicts the multi-model mean. The dotted line indicates 25% changes from 2°C to 1.5°C in global mean temperature.

4. Discussions and Conclusions

In this study, we use a downscaled and bias-corrected CMIP6 ensemble under two continuously-warming scenarios (i.e., SSP245 and SSP585) to address how future global warming would affect the climate ultra-extreme conditions in China. In particular, we consider two global warming levels (1.5°C and 2.0°C) scenarios (SSP245 and SSP585) in order to quantify the potential benefits of slowing down global warming in the context of China. The main conclusions can be summarized as follows:

The bias-corrected CMIP6 models exhibit an outstanding capability in reproducing the historical patterns of maximum, minimum temperature and precipitation over China. The bias-corrected outputs distinctly outperform the raw CMIP6 simulations in capturing the maximum temperature, particularly in northwestern China. The obviously underestimated minimum temperature in raw models across the west and eastward regions is corrected. Likewise, the overall precipitation simulated by raw CMIP6 over China is overvalued completely, and even there

Table 3
The Regional Mean Avoided Impacts of Maximum Temperature, Minimum Temperature, Precipitation and the Corresponding Extreme Indices

Days	TMAX	TMIN	PRE	Extreme hot	Extreme cold	Extreme dry	Extreme wet
SSP245	29.83	40.82	29.14	54.26	18.25	21.17	33.18
SSP585	30.21	27.01	23.33	50.18	14.87	16.87	30.29

Months	Extreme hot-dry	Extreme hot-wet	Extreme cold-dry	Extreme cold-wet
SSP245	29.19	51.35	24.07	56.06
SSP585	41.33	43.17	13.27	33.04

Years	Extreme hot-dry	Extreme hot-wet	Extreme cold-dry	Extreme cold-wet
SSP245	30.52	41.59	15.63	26.78
SSP585	23.46	36.10	11.00	19.06

Note. (unit: %)

is an artificial precipitation center in the Tibet Plateau before correction. These biases and uncertainties among models are reduced efficiently in the process of bias correction.

On the whole of China, the maximum temperature is likely to rise by 1.43°C and 1.97°C, while the regional mean minimum temperature is tended to increase by 1.02°C and 1.83°C at 1.5°C and 2.0°C global warming levels under SSP245 scenario. The magnitude and spatial scope of the increase in minimum temperature with an additional 0.5°C warming are larger than the maximum temperature. The magnitude of precipitation increase over western China will be larger than that in the south, especially for the south of Xinjiang and the west of Tibet. The increment of minimum temperature and precipitation with an extra 0.5°C under SSP585 is smaller than SSP245.

Under the 1.5°C and 2.0°C warming levels, extreme hot conditions would become dominant in most regions of China and some regions are likely to experience over 50 extreme hot days in some regions at future warming levels. The frequency of extreme cold conditions is projected to be smaller than other indices. The utmost occurrent frequency for dry extremes is mainly concentrated over the west of Xinjiang, the southwest of Tibet and southern Sichuan. Future extreme wet events tend to occur in the southeast of Xinjiang and northwest of Tibet under 1.5°C and 2.0°C global warming. We also compared the projections of these ultra-extreme events between raw and bias-corrected results. Relative to the raw output of CMIP6 (Figure S6 in Supporting Information S1), the projected number of univariate ultra-extreme events over China under the different warming levels and scenarios is larger. However, there are some discrepancies between the before and after bias correction in the spatial distributions. For ultra-extreme dry events, the raw GCMs show more frequent extremes would be found in the south of Xinjiang, and the extended region is larger than the results from bias correction.

We analyzed the future co-occurring frequency of four compound extreme indices in the same month and year. More frequent extreme hot-wet events with concurrence in the same month and year would be expected for China under the continuously-warming scenarios. This is particularly obvious for the west where more than 6 hot-wet months are likely to take place under future warming scenarios. This may imply that more extreme heat waves and flooding events would coincide in the same month or year in China in the future. The numbers of concurrence for the cold-dry and cold-wet compound events in the same month or year are quite small, while the extreme hot and dry events are likely to coincide within the same year across China. The differences between the bias-corrected and original output of CMIP6 in projections in concurrent ultra-extreme events in the same month and year are analyzed in Figures S7 and S8in Supporting Information S1. The results show that the northwest of China tends to have more extreme hot-dry events with concurrence in the same month in the future from the raw results. Although the compound hot and wet extremes are more frequent than other indices, the projected overall occurrence frequency is smaller than that in the bias correction. Additionally, two cold-related compound extremes are projected in the local areas (i.e., the western fringes of Tibet) for the bias-corrected results, which are not found in the raw CMIP6. Similar differences are also presented in the projection of the concurrent extreme events in the same year. For the results from bias correction, besides the overall more frequency of concurrence, the local regions are also projected to have more risk to occur these compound extreme events (i.e., cold and dry extremes).

The avoided impacts from 1.5°C to 2.0°C for extreme hot events and extreme wet events are above 25%, particularly for the extreme hot events, the regional mean result is even more than 50%, with 54.26% and 50.18% under SSP245 and SSP585 scenarios. In the same month, the avoided impacts of wet-related extremes will be larger than those of dry-related compound extremes, while the concurrent cold-dry extreme events have less influence (only 13.27% under SSP585) on the added 0.5°C warming. The positive avoided impacts for all univariate and compound extremes suggest that the risk of extreme events over China would decrease robustly when global warming is kept to 1.5°C rather than 2°C under both SSP245 and SSP585. Therefore, it is imperative to keep a lower warming target and continued efforts will offer considerable benefits in terms of minimizing the extreme climate events and their associated socio-economic impacts across China.

Finally, it should be mentioned that there are some unavoidable uncertainties in the projection of future extreme events change. The bias correction approach in this study is one of the uncertainties. Although we have analyzed different probability functions to fit the daily temperature and precipitation distributions and selected the most suitable function to project the frequency of extreme events, the experiments are still limited and it is very necessary to explore the optimal statistical downscaling method in further study, including the other probability functions, improved QM approaches, etc (Guo et al., 2020; Zhu et al., 2022). On the other hand, the methods for defining different warming levels and the thresholds of very extreme or ultra-extreme events also are factors of uncertainty. The timing of reaching global warming levels between CMIP6 models is different, and it may also

be related to internal climate variability (Henley & King, 2017; Smith et al., 2018) and aerosol effects (Dittus et al., 2020) in models. Moreover, as the discussion above, different definitions of extreme percentile thresholds can perform various projections on extreme events in spatial distribution and frequencies of occurrence. Besides, more different climate models and RCP scenarios should be involved in further study to reduce the projection uncertainties.

Data Availability Statement

Data sets analyzed during the current study are available in the Earth System Grid Federation (ESGF) Peer-to-Peer (P2P) distributed data archive (https://aims2.llnl.gov/metagrid/search/?project=CMIP6).

Acknowledgments
This paper is supported by the National Key Research and Development Program of China (Grant 2018YFE0208400), the Science and Technology Project of State Grid Corporation of China (Key Technologies of Novel Integrated Energy System Considering Cross-border Interconnection).

References

Ayugi, B., Tan, G., Ruoyun, N., Babaousmail, H., Ojara, M., Wido, H., et al. (2020). Quantile mapping bias correction on rossby centre regional climate models for precipitation analysis over Kenya, East Africa. *Water*, *12*(3), 801. https://doi.org/10.3390/w12030801

Chen, L., & Frauenfeld, O. W. (2014). A comprehensive evaluation of precipitation simulations over China based on CMIP5 multimodel ensemble projections. *Journal of Geophysical Research: Atmospheres*, *119*(10), 5767–5786. https://doi.org/10.1002/2013jd021190

Chen, S., & Yuan, X. (2021). CMIP6 projects less frequent seasonal soil moisture droughts over China in response to different warming levels. *Environmental Research Letters*, *16*(4), 044053. https://doi.org/10.1088/1748-9326/abe782

CRED. (2022). 2021 disasters in numbers.

de los Milagros Skansi, M., Brunet, M., Sigró, J., Aguilar, E., Groening, J. A. A., Bentancur, O. J., et al. (2013). Warming and wetting signals emerging from analysis of changes in climate extreme indices over South America. *Global and Planetary Change*, *100*, 295–307. https://doi.org/10.1016/j.gloplacha.2012.11.004

Dittus, A. J., Hawkins, E., Wilcox, L. J., Sutton, R. T., Smith, C. J., Andrews, M. B., & Forster, P. M. (2020). Sensitivity of historical climate simulations to uncertain aerosol forcing. *Geophysical Research Letters*, *47*(13), e2019GL085806. https://doi.org/10.1029/2019gl085806

Enayati, M., Bozorg-Haddad, O., Bazrafshan, J., Hejabi, S., & Chu, X. (2021). Bias correction capabilities of quantile mapping methods for rainfall and temperature variables. *Journal of Water and Climate Change*, *12*(2), 401–419. https://doi.org/10.2166/wcc.2020.261

Guo, J., Huang, G., Wang, X., Li, Y., & Yang, L. (2018). Future changes in precipitation extremes over China projected by a regional climate model ensemble. *Atmospheric Environment*, *188*, 142–156. https://doi.org/10.1016/j.atmosenv.2018.06.026

Guo, L., Jiang, Z., Chen, D., Le Treut, H., & Li, L. (2020). Projected precipitation changes over China for global warming levels at 1.5°C and 2°C in an ensemble of regional climate simulations: Impact of bias correction methods. *Climatic Change*, *162*(2), 623–643. https://doi.org/10.1007/s10584-020-02841-z

Henley, B. J., & King, A. D. (2017). Trajectories toward the 1.5 C Paris target: Modulation by the interdecadal Pacific oscillation. *Geophysical Research Letters*, *44*(9), 4256–4262. https://doi.org/10.1002/2017gl073480

Hirota, N., & Takayabu, Y. N. (2013). Reproducibility of precipitation distribution over the tropical oceans in CMIP5 multi-climate models compared to CMIP3. *Climate Dynamics*, *41*(11–12), 2909–2920. https://doi.org/10.1007/s00382-013-1839-0

IPCC. (2018). Summary for policymakers. In V. Masson-Delmotte, P. Zhai, H.-O. Pörtner, D. Roberts, J. Skea, et al. (Eds.), *Global warming of 1.5°C. An IPCC special report on the impacts of global warming of 1.5°C above pre-industrial levels and related global greenhouse gas emission pathways, in the context of strengthening the global response to the threat of climate change, sustainable development, and efforts to eradicate poverty* (pp. 3–24).

Jia, W., & Xue-Jie, G. (2013). A gridded daily observation dataset over China region and comparison with the other datasets (in Chinese). *Chinese Journal of Geophysics Chinese Edition*, *56*, 1102–1111.

Jiang, Z., Li, W., Xu, J., & Li, L. (2015). Extreme precipitation indices over China in CMIP5 models. Part I: Model evaluation. *Journal of Climate*, *28*(21), 8603–8619. https://doi.org/10.1175/jcli-d-15-0099.1

Kim, J. B., & Bae, D. H. (2021). The impacts of global warming on climate zone changes over Asia based on CMIP6 projections. *Earth and Space Science*, *8*, e2021EA001701. https://doi.org/10.1029/2021ea001701

Kim, Y.-H., Min, S.-K., Zhang, X., Sillmann, J., & Sandstad, M. (2020). Evaluation of the CMIP6 multi-model ensemble for climate extreme indices. *Weather and Climate Extremes*, *29*, 100269. https://doi.org/10.1016/j.wace.2020.100269

Li, D., Qi, Y., & Zhou, T. (2021). Changes in rainfall erosivity over mainland China under stabilized 1.5°C and 2°C warming futures. *Journal of Hydrology*, *603*, 126996. https://doi.org/10.1016/j.jhydrol.2021.126996

Li, D., Zhou, T., Zou, L., Zhang, W., & Zhang, L. (2018). Extreme high-temperature events over East Asia in 1.5°C and 2°C warmer futures: Analysis of NCAR CESM low-warming experiments. *Geophysical Research Letters*, *45*(3), 1541–1550. https://doi.org/10.1002/2017gl076753

Li, H., Sheffield, J., & Wood, E. F. (2010). Bias correction of monthly precipitation and temperature fields from intergovernmental panel on climate change AR4 models using equidistant quantile matching. *Journal of Geophysical Research*, *115*(D10), D10101. https://doi.org/10.1029/2009jd012882

Liu, C., Yang, C., Yang, Q., & Wang, J. (2021). Spatiotemporal drought analysis by the standardized precipitation index (SPI) and standardized precipitation evapotranspiration index (SPEI) in Sichuan Province, China. *Scientific Reports*, *11*, 1–14. https://doi.org/10.1038/s41598-020-80527-3

Lu, Y., Hu, H., Li, C., & Tian, F. (2018). Increasing compound events of extreme hot and dry days during growing seasons of wheat and maize in China. *Scientific Reports*, *8*, 1–8. https://doi.org/10.1038/s41598-018-34215-y

Meng, Y., Hao, Z., Feng, S., Zhang, X., & Hao, F. (2022). Increase in compound dry-warm and wet-warm events under global warming in CMIP6 models. *Global and Planetary Change*, *210*, 103773. https://doi.org/10.1016/j.gloplacha.2022.103773

Mishra, V., Bhatia, U., & Tiwari, A. D. (2020). Bias-corrected climate projections for South Asia from coupled model intercomparison project-6. *Scientific Data*, *7*, 1–13. https://doi.org/10.1038/s41597-020-00681-1

Morsy, M., & El Afandi, G. (2021). Decadal changes of heatwave aspects and heat index over Egypt. *Theoretical and Applied Climatology*, *146*(1–2), 71–90. https://doi.org/10.1007/s00704-021-03721-x

Piao, J., Chen, W., Wang, L., & Chen, S. (2022). Future projections of precipitation, surface temperatures and drought events over the monsoon transitional zone in China from bias-corrected CMIP6 models. *International Journal of Climatology*, *42*(2), 1203–1219. https://doi.org/10.1002/joc.7297

Ridder, N. N., Pitman, A. J., Westra, S., Ukkola, A., Do, H. X., Bador, M., et al. (2020). Global hotspots for the occurrence of compound events. *Nature Communications*, *11*, 1–10. https://doi.org/10.1038/s41467-020-19639-3

Shi, Z., Jia, G., Zhou, Y., Xu, X., & Jiang, Y. (2021). Amplified intensity and duration of heatwaves by concurrent droughts in China. *Atmospheric Research*, *261*, 105743. https://doi.org/10.1016/j.atmosres.2021.105743

Smith, D., Scaife, A., Hawkins, E., Bilbao, R., Boer, G., Caian, M., et al. (2018). Predicted chance that global warming will temporarily exceed 1.5 C. *Geophysical Research Letters*, *45*(21), 11895–11903. https://doi.org/10.1029/2018gl079362

Sobral, B. S., de Oliveira-Junior, J. F., de Gois, G., Pereira-Júnior, E. R., de Bodas Terassi, P. M., Muniz-Júnior, J. G. R., et al. (2019). Drought characterization for the state of Rio de Janeiro based on the annual SPI index: Trends, statistical tests and its relation with ENSO. *Atmospheric Research*, *220*, 141–154. https://doi.org/10.1016/j.atmosres.2019.01.003

Su, B., Huang, J., Mondal, S. K., Zhai, J., Wang, Y., Wen, S., et al. (2021). Insight from CMIP6 SSP-RCP scenarios for future drought characteristics in China. *Atmospheric Research*, *250*, 105375. https://doi.org/10.1016/j.atmosres.2020.105375

Sun, W., Mu, X., Song, X., Wu, D., Cheng, A., & Qiu, B. (2016). Changes in extreme temperature and precipitation events in the Loess Plateau (China) during 1960–2013 under global warming. *Atmospheric Research*, *168*, 33–48. https://doi.org/10.1016/j.atmosres.2015.09.001

Tang, B., Hu, W., Duan, A., Gao, K., & Peng, Y. (2022). Reduced risks of temperature extremes from 0.5°C less global warming in the Earth's three Poles. *Earth's Future*, *10*(2), e2021EF002525. https://doi.org/10.1029/2021ef002525

Taylor, K. E. (2001). Summarizing multiple aspects of model performance in a single diagram. *Journal of Geophysical Research*, *106*(D7), 7183–7192. https://doi.org/10.1029/2000jd900719

Tian, J., Zhang, Z., Ahmed, Z., Zhang, L., Jiang, T., & Tao, H. (2021). Projections of precipitation over China based on CMIP6 models. *Stochastic Environmental Research and Risk Assessment*, *35*(4), 1–18. https://doi.org/10.1007/s00477-020-01948-0

Tokarska, K. B., Stolpe, M. B., Sippel, S., Fischer, E. M., Smith, C. J., Lehner, F., & Knutti, R. (2020). Past warming trend constrains future warming in CMIP6 models. *Science Advances*, *6*(12), eaaz9549. https://doi.org/10.1126/sciadv.aaz9549

Vogel, M. M., Hauser, M., & Seneviratne, S. I. (2020). Projected changes in hot, dry and wet extreme events' clusters in CMIP6 multi-model ensemble. *Environmental Research Letters*, *15*(9), 094021. https://doi.org/10.1088/1748-9326/ab90a7

Wang, B., Zhang, M., Wei, J., Wang, S., Li, S., Ma, Q., et al. (2013). Changes in extreme events of temperature and precipitation over Xinjiang, northwest China, during 1960–2009. *Quaternary International*, *298*, 141–151. https://doi.org/10.1016/j.quaint.2012.09.010

Wang, L., & Chen, W. (2014). Equiratio cumulative distribution function matching as an improvement to the equidistant approach in bias correction of precipitation. *Atmospheric Science Letters*, *15*, 1–6. https://doi.org/10.1002/asl2.454

Wei, L., Liu, L., Jing, C., Wu, Y., Xin, X., Yang, B., et al. (2022). Simulation and projection of climate extremes in China by a set of statistical downscaled data. *International Journal of Environmental Research and Public Health*, *19*(11), 6398. https://doi.org/10.3390/ijerph19116398

Xu, F., & Luo, M. (2019). Changes of concurrent drought and heat extremes in the arid and semi-arid regions of China during 1961–2014. *Atmospheric Science Letters*, *20*(12), e947. https://doi.org/10.1002/asl.947

Yang, L., Tian, J., Fu, Y., Zhu, B., He, X., Gao, M., et al. (2022). Will the arid and semi-arid regions of Northwest China become warmer and wetter based on CMIP6 models? *Hydrology Research*, *53*(1), 29–50. https://doi.org/10.2166/nh.2021.069

Yang, X., Wood, E. F., Sheffield, J., Ren, L., Zhang, M., & Wang, Y. (2018). Bias correction of historical and future simulations of precipitation and temperature for China from CMIP5 models. *Journal of Hydrometeorology*, *19*(3), 609–623. https://doi.org/10.1175/jhm-d-17-0180.1

Ying-Xue, L., Chang-Chun, X., Zhi, C., Qi, S., & Li, C. (2020). Application of CN05. 1 meteorological data in watershed hydrological simulation: A case study in the upper reaches of Kaidu river basin. *Advances in Climate Change Research*, *16*, 287.

You, M., & Liu, P. (2022). The carbon puzzle: Examining the impact of China's "30● 60 dual-carbon target" on carbon-intensive and green firms. Available at SSRN 4016959.

Yu, R., & Zhai, P. (2020). Changes in compound drought and hot extreme events in summer over populated eastern China. *Weather and Climate Extremes*, *30*, 100295. https://doi.org/10.1016/j.wace.2020.100295

Zhang, H., Wu, C., Yeh, P. J. F., & Hu, B. X. (2020). Global pattern of short-term concurrent hot and dry extremes and its relationship to large-scale climate indices. *International Journal of Climatology*, *40*(14), 5906–5924. https://doi.org/10.1002/joc.6555

Zhao, J.-T., Su, B.-D., Wang, Y.-J., Tao, H., & Jiang, T. (2021). Population exposure to precipitation extremes in the Indus River Basin at 1.5°C, 2.0°C, and 3.0°C warming levels. *Advances in Climate Change Research*, *12*(2), 199–209. https://doi.org/10.1016/j.accre.2021.03.005

Zhou, P., & Liu, Z. (2018). Likelihood of concurrent climate extremes and variations over China. *Environmental Research Letters*, *13*(9), 094023. https://doi.org/10.1088/1748-9326/aade9e

Zhu, H., Jiang, Z., & Li, L. (2021). Projection of climate extremes in China, an incremental exercise from CMIP5 to CMIP6. *Science Bulletin*, *66*(24), 2528–2537. https://doi.org/10.1016/j.scib.2021.07.026

Zhu, L., Kang, W., Li, W., Luo, J.-J., & Zhu, Y. (2022). The optimal bias correction for daily extreme precipitation indices over the Yangtze-Huaihe River Basin, insight from BCC-CSM1. 1-m. *Atmospheric Research*, *271*, 106101. https://doi.org/10.1016/j.atmosres.2022.106101